Inactivation Viewed Through Single Sodium Channels

CAROL A. VANDENBERG and RICHARD HORN

From the Department of Physiology, University of California at Los Angeles School of Medicine, Los Angeles, California 90024

ABSTRACT Recordings of the sodium current in tissue-cultured GH_3 cells show that the rate of inactivation in whole cell and averaged single channel records is voltage dependent: τ_h varied e-fold/~26 mV. The source of this voltage dependence was investigated by examining the voltage dependence of individual rate constants, estimated by maximum likelihood analysis of single channel records, in a five-state kinetic model. The rate constant for inactivating from the open state, rather than closing, increased with depolarization, as did the probability that an open channel inactivates. The rate constant for closing from the open state had the opposite voltage dependence. Both rate constants contributed to the mean open time, which was not very voltage dependent. Both open time and burst duration were less than τ_h for voltages up to −20 mV. The slowest time constant of activation, τ_m, was measured from whole cell records, by fitting a single exponential either to tail currents or to activating currents in trypsin-treated cells, in which the inactivation was abolished. τ_m was a bell-shaped function of voltage and had a voltage dependence similar to τ_h at voltages more positive than −35 mV, but was smaller than τ_h. At potentials more negative than about −10 mV, individual channels may open and close several times before inactivating. Therefore, averaged single channel records, which correspond with macroscopic current elicited by a depolarization, are best described by a convolution of the first latency density with the autocorrelation function rather than with 1 − (channel open time distribution). The voltage dependence of inactivation from the open state, in addition to that of the activation process, is a significant factor in determining the voltage dependence of macroscopic inactivation. Although the rates of activation and inactivation overlapped greatly, independent and coupled inactivation could not be statistically distinguished for two models examined. Although rates of activation affect the observed rate of inactivation at intermediate voltages, extrapolation of our estimates of rate constants suggests that at very depolarized voltages the activation process is so fast that it is an insignificant factor in the time course of inactivation. Prediction of gating currents shows that an inherently voltage-dependent inactivation process need not produce a conspicuous component in the gating current.

Address reprint requests to Dr. Richard Horn, Dept. of Physiology, UCLA School of Medicine, Center for the Health Sciences, Los Angeles, CA 90024.

J. GEN. PHYSIOL. © The Rockefeller University Press · 0022-1295/84/10/0535/30 $1.00 535
Volume 84 October 1984 535–564

INTRODUCTION

Voltage clamp experiments of macroscopic sodium currents clearly show that inactivation is voltage dependent (Hodgkin and Huxley, 1952). Steady state inactivation, measured by standard h_∞ experiments, and rates of inactivation, measured by single or double pulse protocols, are both strongly voltage dependent. These measurements of inactivation have recently been compared with measurements obtained from gating currents and single channel recording (see reviews in Armstrong, 1981; Bezanilla, 1982; French and Horn, 1983). The motivation for these comparisons, in part, is to find the source of the voltage dependence of inactivation.

In the original formulation of Hodgkin and Huxley, inactivation was assumed to have its own voltage dependence and to function independently of activation, the process responsible for opening of resting channels. In the past decade, however, increasing evidence points to the possibility that inactivation is not inherently voltage dependent, but only appears so because of coupling with activation (Armstrong, 1981; Bezanilla, 1982; French and Horn, 1983). In the simplest version of coupling, a channel must open before being able to inactivate. The faster a channel can open, the faster it can inactivate by a mechanism that is possibly voltage independent. Considerable experimental data are in accordance with this hypothesis, although it is now generally accepted that closed channels can also inactivate without opening (Bean, 1981; Horn et al., 1981; Aldrich et al., 1983; Aldrich and Stevens, 1983; Patlak, 1983; Horn and Vandenberg, 1984).

One approach to describing the interaction between activation and inactivation is the simple presentation of estimated rate constants for a given kinetic model at each membrane potential (e.g., see Tables I and III in Horn and Vandenberg, 1984), since all rate constants, in principle, affect the observed rate of the decay of macroscopic currents (Colquhoun and Hawkes, 1977; French and Horn, 1983). For the sake of clarity, we call this decay "macroscopic inactivation." Its rate represents one or a weighted sum of eigenvalues associated with a kinetic model. We distinguish this decay rate from "microscopic inactivation," the rate constant(s) responsible for transitions into an inactivated conformation. Specifically, we will concentrate on the rate constants β_I for the transition between the open state and an inactivated state and β_A for the return to the last closed state from the open state (cf. Aldrich and Stevens, 1983; Aldrich et al., 1983; Horn et al., 1984; Horn and Vandenberg 1984). A tabulation of estimated rate constants provides little insight, unfortunately, into the interaction between activation and macroscopic inactivation. It would be desirable to have a simple physical interpretation of single channel behavior that would provide an approximation to the eigenvalue(s) represented in macroscopic inactivation and which might describe which eigenvalue(s) should be identified with macroscopic inactivation. We have examined four simple mechanisms that are possible representations of this interaction and provide a conceptual framework beyond the simple listing of rate constants.

Mechanism 1: Macroscopic inactivation is determined by the dwell time in the open state. In this scheme, channels open rapidly after a step depolarization.

When the current reaches a peak, activation is essentially complete, and thereafter channels close slowly by randomly entering an inactivated conformation. Partial support for this mechanism comes from experiments in squid axon, where pharmacological removal of inactivation has little effect on the time course of activation or the peak current at a given voltage (e.g., see Bezanilla and Armstrong, 1977; Oxford, 1981). If mechanism 1 is correct, the mean open time will have approximately the same value and voltage dependence as τ_h, the time constant of macroscopic inactivation. Since channels will only open once before inactivating, β_I will be much larger than other rate constants leaving the open state, and its inverse will be approximately equal to τ_h.

Mechanism 2: Macroscopic inactivation is determined by the mean burst duration. In this mechanism, channels open rapidly after a depolarizing voltage step and burst for a random duration, which is significantly longer than the rapid activation. Many transitions can contribute to the burst duration because it reflects open and closed times as well as the number of openings in a burst. This is somewhat similar to the proposed mechanism underlying the decay of the endplate current in skeletal muscle (Colquhoun and Sakmann, 1981). If this scheme is correct, the mean burst duration will have approximately the same value and voltage dependence as τ_h. Both mechanisms 1 and 2 assume that channels open rapidly after a depolarization, but differ in the relative rates β_I and β_A for transitions from the open state: mechanism 1 implies that $\beta_I \gg \beta_A$, and mechanism 2 that they are either of comparable magnitude or that $\beta_A > \beta_I$. However, in mammalian cells, single channels may open slowly after a depolarization (Horn et al., 1981, 1984; Patlak and Horn, 1982; Aldrich et al., 1983; Aldrich and Stevens, 1983; French and Horn, 1983), which is not in accord with these mechanisms.

Mechanism 3: The time course of macroscopic inactivation is mainly determined by coupling with activation. In this mechanism, the apparent rate of inactivation is determined by the rate at which channels approach or reach the open state, and not by open time or burst duration, which are small by comparison with time constants of activation. This idea has support from both axon experiments and single channel recordings (see reviews of Armstrong, 1981; Bezanilla, 1982; French and Horn, 1983). Aldrich et al. (1983) and Aldrich and Stevens (1983) proposed that the time course and voltage dependence of macroscopic inactivation are primarily a function of the first latency distribution, and that open channels close rapidly into an inactivated conformation. If this scheme is correct, the times when channels first reach the open state after a depolarizing step will be distributed throughout the decaying phase of macroscopic currents.

Mechanism 4: The time course of macroscopic inactivation depends on both activation and burst duration. This is the most general case and is a direct consequence of the fact that the sodium channel has one open state (Horn and Vandenberg, 1984). In such a channel, the activation process, β_I, and β_A all have comparable rates and the probabilities of transitions along these pathways overlap temporally so that they all contribute to macroscopic inactivation. If channels briefly open only once, instead of bursting, then mechanism 3 is a sufficient description of gating. If the rate of activation, reflected by the first latency

density, is much faster than macroscopic inactivation, then one of the first two schemes is more appropriate.

For all four mechanisms, if a channel has one open state, then the convolution of the first latency density with the autocorrelation function for an open channel will reproduce $P_{open}(t)$, the probability of a channel being open after the onset of a step depolarization (Aldrich et al., 1983). However, for the limiting cases described by mechanisms 1 and 2, when activation is much faster than inactivation, $P_{open}(t)$ will be approximatedly equal to $L(t)$ or the autocorrelation, respectively, where $L(t) = 1 -$ (open time distribution function) is the probability that a channel, open at time zero, is still open at time t. As activation becomes rate limiting in mechanism 3, $P_{open}(t)$ can be described by a convolution of the first latency density and $L(t)$, or if the open time is very short, by the first latency density alone.

In this paper, we first examine the macroscopic properties of inactivation in GH_3 cells, and then explore the predictions of the preceding mechanisms in turn. Our results will suggest that the appropriate mechanism depends on membrane potential.

METHODS

The methods used for single channel recording and data analysis are described in Horn and Vandenberg (1984), except where noted below.

Whole cell recording methods follow the general techniques described in Marty and Neher (1983) and Fernandez et al. (1984). We used large pipettes for these experiments (<2 MΩ resistance in the bath) and selected small cells (diameter less than ~15 μm), to ensure both rapid exchange of our pipette solution with the cytoplasm and optimal electrical properties. In some experiments, series resistance compensation was used, especially to correct the effects of current passing between the pipette and the cell interior. This usually caused a minimal effect on the time course or magnitude of the currents when compensating with values of two to three times the electrode resistance in the bath (see Horn and Brodwick, 1980; Fernandez et al., 1984). Series resistance compensation also had a minimal effect on the rapid kinetics of activation when the capacitative current caused by charging the cell membrane was allowed to pass through the series resistance circuit (Sigworth, 1983). We selected cells that were loosely attached to the substrate and lifted them with the recording electrode to the surface of the bath to reduce noise and capacitative transients caused by coupling between the pipette and the bath. Linear capacitance and leakage currents were removed from the macroscopic currents by the $P/-4$ procedure (see Bezanilla and Armstrong, 1977). The scaled averages of 16 hyperpolarizing pulses of amplitude $P/4$, where P is the difference between the test potential and the holding potential, were taken from a subtracting holding potential of −70 mV and then added to the test pulse current. We usually waited at least 1 h before making recordings to allow the parameters of activation and inactivation to shift (Fenwick et al., 1982; Marty and Neher, 1983; Fernandez et al., 1984). Whole cell currents were low-pass-filtered at 2.5–3 kHz.

In several experiments, trypsin (TPCK-treated, type XIII, Sigma Chemical Co., St. Louis, MO) was added to the recording pipette to remove inactivation in both single channel records and whole cell recording. This reagent was preferable to *N*-bromoacetamide, which we had used previously (Horn et al., 1984), as we describe below. All experiments were performed at 9.3°C.

Data analysis followed the techniques described in Horn and Vandenberg (1984). We

fit single exponentials to the decay of macroscopic currents in single pulse experiments for both whole cell and averaged single channel records, and to tail currents in control and trypsin-treated experiments, using a nonlinear least-squares fit with the Powell (1978) algorithm mentioned in the preceding paper. The time constant and amplitude of the exponential and the baseline were free parameters in these fits. This method was also used to fit theoretical curves to h_∞ measurements. Single exponential fits to the activation of trypsin-treated whole cell currents were made by eye. Mean open time, t_o, in multi-channel patches was estimated as

$$t_o = \sum_i n_i T_i / n,$$

where T_i is the duration of n_i open channels and n is the total number of closing transitions in the experimental records (Fenwick et al., 1982; Horn and Lange, 1983; Horn et al., 1984).

RESULTS

The voltage dependence of the rate of macroscopic inactivation is evident in Fig. 1*A*, which shows whole cell sodium currents in response to voltage steps from −80 mV to a series of test potentials in 10-mV increments. At all but the most negative potentials, the currents decay nearly to zero by the end of the 29-ms record. The rate of decay was measured by fitting a single exponential with time constant τ_h to the falling phase of the current, as shown in Fig. 1*B*, which shows the best fits at −20, 0, and +20 mV. It is clear from the raw records, as well as

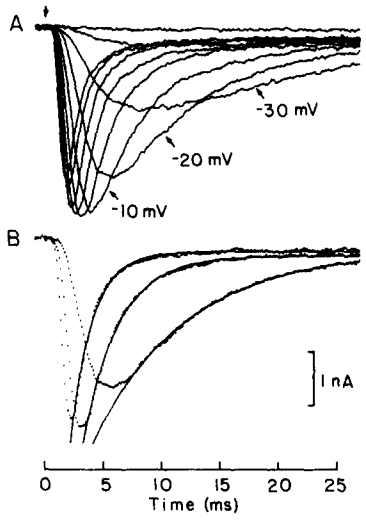

FIGURE 1. Macroscopic sodium currents from whole cell recording. (*A*) Currents were elicited in response to 29-ms voltage steps to test potentials from −50 to +40 mV in 10-mV increments from a holding potential of −80 mV. (*B*) Currents for test pulses to −20, 0, and +20 mV (dotted line) from *A* plotted together with single exponential fits to the falling phase of the currents (solid curve). τ_h is 8.1 (−20 mV), 3.1 (0 mV), and 1.9 ms (+20 mV). Each trace is the average of eight records, corrected for leakage and capacitative currents. The interpulse interval was 1.0 s, filtered at 3 kHz.

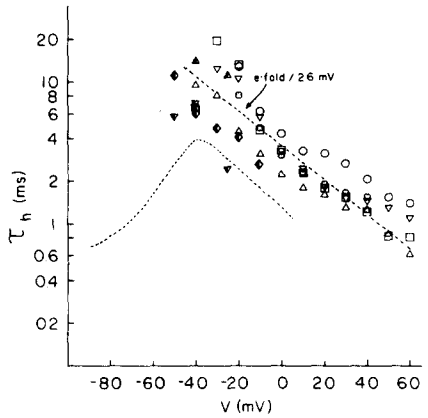

FIGURE 2. τ_h vs. voltage. τ_h, the time constant of macroscopic inactivation, was obtained by fitting a single exponential to the falling phase of macroscopic currents, as shown in Fig. 1*B*. Open symbols are from whole cell records, and half-filled symbols represent fits to averaged single channel records. The dashed line through the data was drawn by eye. The lower curved line shows τ_m vs. voltage from Fig. 10.

from the plot of τ_h vs. potential (Fig. 2), that the rate of macroscopic inactivation is increased by depolarization over this voltage range. The same fitting procedure is easily applied to averaged single channel records (cf. Aldrich et al., 1983), and these values of τ_h are also plotted in Fig. 2 as half-filled symbols. Over the voltage range in which these measurements overlap, the time constants for whole cell and averaged single channel currents generally agree, as found by Fernandez et

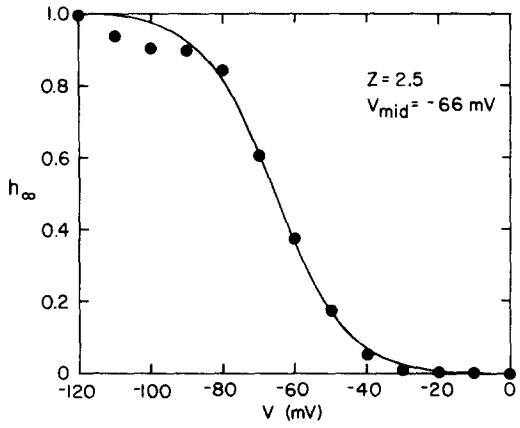

FIGURE 3. h_∞ vs. voltage. The steady state level of fast inactivation was determined by the peak current elicited by a test pulse to −25 mV following a 100-ms prepulse to the indicated voltage from a holding potential of −110 mV. The values represent the average of four consecutive records from a whole cell experiment. The theoretical curve is a fit to the Boltzmann distribution, which had a midpoint at −66 mV and the equivalent voltage dependence of 2.5 charges moving across the membrane field. The interpulse interval was 1.0 s.

al. (1984), although the single channel currents are somewhat shifted (by ~10 mV) in the hyperpolarized direction in our experiments. The straight line shown in Fig. 2 has a slope of e-fold/26 mV, which is similar to that seen in squid axon (Fig. 5 in Bezanilla and Armstrong, 1977). The lower dashed curve in Fig. 2 represents τ_m, the time constant for activation, as discussed later.

Fig. 3 shows a standard h_∞ curve for a whole cell experiment. This is an estimate of the steady state voltage dependence of fast inactivation. The data show the relative values of peak current for a step to −25 mV vs. the voltage level of a preceding 100-ms prepulse. The theoretical Boltzmann distribution was determined statistically by unweighted least-squares regression and had a midpoint of −66 mV and a voltage dependence equivalent to 2.5 electronic charges moving all the way through the membrane field, which is equivalent to e-fold/10 mV. This voltage dependence was similar in all cells, but the midpoint of the h_∞ curve was variable between cells, in the range of −95 to −60 mV.

Figs. 2 and 3 show that macroscopic inactivation in this preparation is voltage dependent in both its kinetic and its steady state nature. In the next section, we examine the voltage dependence of β_I, the rate constant for inactivation (i.e., microscopic inactivation) from the open state. Specifically, we will examine whether $1/\beta_I$ is equivalent to τ_h, as predicted by mechanism 1 (see above).

Microscopic Inactivation Is Voltage Dependent

Because of the possibility of making statistical tests and defining confidence intervals, we estimated β_I in our patches with the maximum likelihood method described in Horn and Vandenberg (1984). We examined a total of four patches using this method. Two patches contained two channels, one contained one channel, and the last contained four channels. We used the following model, which is similar to the basic model described in Horn and Vandenberg (1984):

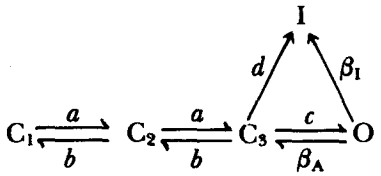

(Scheme 1)

Although this model has irreversible inactivation, and is therefore not statistically as good as the basic model, the latter required unreasonable computation times in multichannel patches. Furthermore, the estimates of β_I were essentially the same for the two models whenever we compared them. Another modification from the procedure in Horn and Vandenberg (1984) was necessary in our multichannel patches because these patches showed evidence of either hibernation or resting inactivation (Horn et al., 1984; Horn and Vandenberg, 1984), based on runs analysis and the fact that the inclusion of a hibernating state improved the log(likelihood)s (see Table V in Horn and Vandenberg, 1984). The effect of this modification was minimal on estimates of β_I at relatively depolarized voltages, but always tended to increase the magnitude of the estimates at negative voltages. Therefore, this modification tends to decrease the apparent voltage dependence of β_I.

Fig. 4*A* shows the maximum likelihood estimates of β_I for these patches, along with their estimated standard errors. Each symbol corresponds to a different experiment. Inspection of the standard errors shows that the estimates were

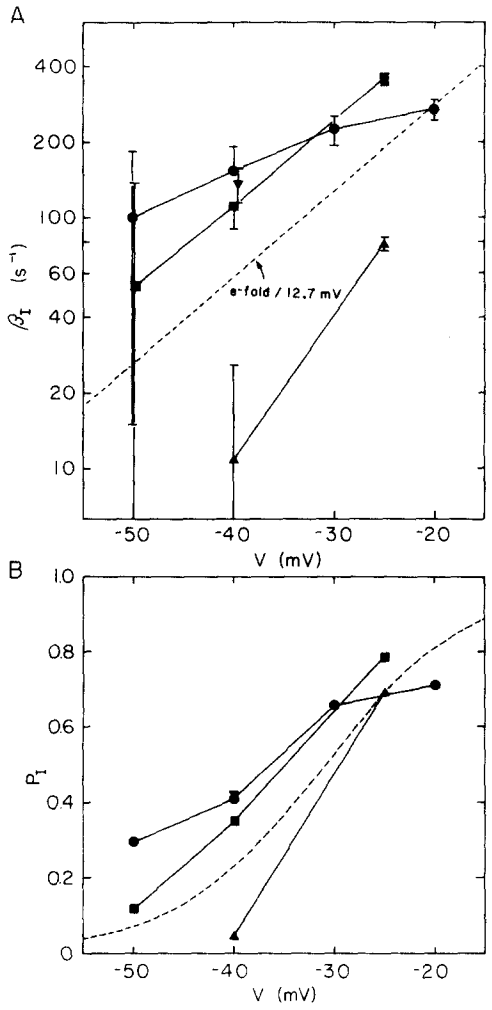

FIGURE 4. Rate constant for inactivating from the open state, β_I, and probability of an open channel inactivating, P_I, vs. voltage. (*A*) β_I and its standard error (error bars) were estimated using Scheme 1 by maximum likelihood analysis of single channel current records from outside-out patches containing from one to four channels. Each type of symbol represents a particular patch: ●, experiment 28 (four channels); ▼, experiment 50 (two channels); ▲, experiment 56 (one channel); ■, experiment 67 (two channels). The dashed line, with a voltage dependence of e-fold/12.7 mV, is an average of weighted log-linear regression lines for the three experiments. (*B*) The probability that an open channel inactivates rather than closes, P_I, was calculated from the estimated rate constants for an open channel inactivating, β_I (*A*), and closing, β_A (Fig. 5). The dashed line is the theoretical prediction using the regression lines in *A* and Fig. 5.

more reliable at relatively depolarized voltages. For the three patches where measurements were obtained at more than one voltage, we estimated the voltage dependence of β_I by weighted log-linear regression (Rao, 1973), using both the standard errors and the semilog relationship to obtain weighting factors. For the three experiments, the regression slopes were equivalent to voltage dependences of e-fold for 7.6, 38.3, and 12.8 mV. The average regression line is shown in Fig. 4*A* and has a slope of e-fold/12.7 mV.

Fig. 5 shows estimates of the closing rate constant, β_A, in the same experiments. The regression line here has a slope of e-fold/18.7 mV. β_A decreases with depolarization, as expected (e.g., see Hodgkin and Huxley, 1952) and as previously estimated from experiments in which inactivation was removed pharmacologically (Horn et al., 1984). The estimates of β_I and β_A immediately lead to estimates of $P_I = \beta_I/(\beta_I + \beta_A)$, as shown in Fig. 4*B*. The dashed sigmoidal curve is obtained from the rate constants given by the regression lines in Figs. 4*A* and 5. This graph shows that an open channel tends to "close" at hyperpolarized and "inactivate" at depolarized potentials, as we previously suggested from experiments using *N*-bromoacetamide (Horn et al., 1984).

We were also interested in the voltage dependence of inactivation from closed states. Unfortunately, these rate constants were highly variable between patches and also very model dependent. It is clear from our h_∞ estimates (Fig. 3), however, that closed channel inactivation is voltage dependent, in agreement with single channel experiments of Aldrich and Stevens (1983).

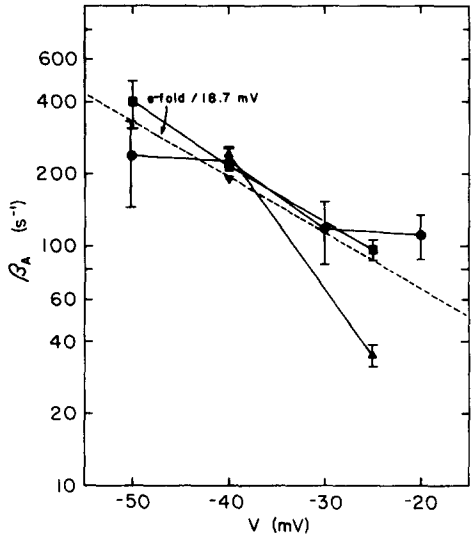

FIGURE 5. Rate constant for closing from the open state, β_A, vs. voltage. β_A and its standard error (error bars) were estimated by maximum likelihood analysis of single channel current records. The dashed line, with a slope of e-fold/18.7 mV, was obtained by log-linear regression. The symbols correspond with the same experiments plotted in Figs. 4 and 6.

Statistical Tests of the Voltage Dependence of β_I

Because of the large standard errors of the estimates of β_I, especially at hyperpolarized voltages, it is worthwhile considering the reliability of our conclusion that β_I is voltage dependent. First, we ask this question of the data presented in Fig. 4*A*. Then we will consider other tests of the voltage dependence of β_I.

In one patch, data were obtained at only two voltages, −25 and −40 mV. Large sample theory ensures that the maximum likelihood estimates have a normal distribution, and we tested the null hypothesis that the means of the estimates at these two voltages were the same (cf. Rao, 1973). In this patch, the estimates were 77.96 ± 5.04 s^{-1} at −25 mV and 10.77 ± 15.23 s^{-1} at −40 mV, which are significantly different ($P \sim 5 \times 10^{-5}$). In two other patches, estimates were obtained at more than two voltages. In these cases, a t test was applied under the null hypothesis that the weighted log-linear regression slopes were zero. The t values were 20.80 (degrees of freedom = 1) and 6.32 (degrees of freedom = 2) in the two experiments, and the null hypothesis was rejected for both ($P < 0.02$). Therefore, these estimates all show a significant voltage dependence.

Another test for the voltage dependence of β_I can be obtained by a simultaneous estimation of all rate constants at all voltages, with the constraint that β_I be the same at each voltage. The maximum likelihood value for this constrained fit can be compared with that of the unconstrained fit by use of a likelihood ratio test. Unfortunately, this straightforward calculation is computationally infeasible because of the long time required to estimate 11 rate constants for a very large data set. Instead, we examined constrained fits for a few selected values of β_I. We used three values with data from the patch with one channel. The values were 77.96, 10.77, and 44.37 s^{-1}, which are the unconstrained estimates at −25 and −40 mV and the average of the two estimates, respectively. The likelihood ratio tests for these values of β_I yielded chi-square (degrees of freedom = 2) values of 177.57, 331.30, and 196.89, respectively, which shows that the constrained estimates are significantly poorer than the unconstrained estimates ($P < 10^{-4}$). Again, β_I is significantly voltage dependent.

The estimates of β_I are, not surprisingly, model dependent. Although we chose scheme 1 because of its statistical qualities (Horn and Vandenberg, 1984), other models show different voltage dependencies for estimates of β_I. This is partly because of the fact that the rates of closed channel inactivation affect maximum likelihood estimates of β_I. The reliability of these estimates is especially apparent at hyperpolarized voltages and is, therefore, quite model dependent there. For the one-channel patch examined in this paper and in Horn and Vandenberg (1984), β_I was determined in 23 models. Although the kinetic schemes often were very different from one another, β_I had approximately the same value in all models at −25 mV (82.1 ± 3.6 s^{-1}, mean ± standard deviation). At −40 mV, the estimates were more model dependent (β_I = 34.2 ± 28.5 s^{-1}). For every model, β_I was increased by depolarization, with a voltage dependence for the above mean values of e-fold/17.2 mV. Thus, by all criteria, β_I is increased by depolarization.

Analysis by the ACS Method Predicts the Voltage Dependence of Microscopic Inactivation

We have also analyzed our single channel data using the approach of Aldrich, Corey, and Stevens, the "ACS" method (Aldrich et al., 1983; Aldrich and Stevens, 1983). We assume their simple model, that a channel has three states, one open (O) and two closed (C and I), arranged as follows:

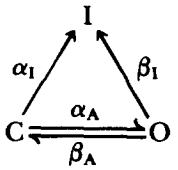

where the channel at rest is in state C. Depolarization eventually leads to inactivation, either by path C → I or by path O → I. We define the following probabilities, $P(i \rightarrow j)$, which refer to the probability that a channel next enters state j after leaving state i (Aldrich et al., 1983):

$$\text{Prob } (C \rightarrow O) = P_o$$
$$\text{Prob } (C \rightarrow I) = 1 - P_o$$
$$\text{Prob } (O \rightarrow I) = P_I$$
$$\text{Prob } (O \rightarrow C) = 1 - P_I.$$

Aldrich and Stevens (1983) showed that the average number, K, of openings per record for this scheme is given by

$$K = NP_o/[1 - P_o(1 - P_I)], \tag{1}$$

where N is the number of channels in the patch. Rearranging gives

$$P_I = (K + N)/K - 1/P_o. \tag{2}$$

We estimate $1 - P_o$ as the Nth root of the fraction of blank traces, and K is the measured average number of openings per record.

Table I shows the results of this analysis for two patches, one with a single channel, the second with two channels. The left side of Table I shows estimates of P_o, P_I, and β_I using the ACS method (Aldrich et al., 1983; Aldrich and Stevens, 1983). β_I is obtained by dividing P_I by the average open time at each voltage. For both patches, P_o increases with depolarization. This is an expected consequence of the voltage dependence of activation, since depolarization increases α_A, the rate constant for channel opening, and increases the probability of a closed channel opening before inactivating. Also, depolarization increases P_I for both patches. However, the ACS estimate of P_I was negative at −40 mV in the patch with two channels. The negative estimate of a probability is due to the fact that P_I in Eq. 2 is not constrained. When P_o is small, P_I can be negative. For positive values of P_I, we could estimate β_I, which, at least in the case of the one-channel patch, was voltage dependent, increasing e-fold/12.5 mV.

We used the above three-state model (model 21 in Horn and Vandenberg, 1984), and estimated the four rate constants for both experiments by the

TABLE I

Comparison of ACS and MLE Methods

		Experiment 56 (One channel)					
		ACS method			MLE method		
V	K	P_o	P_I	β_I	P_o	P_I	β_I
mV				s^{-1}			s^{-1}
−25	1.00	0.77	0.701	79.7	0.77	0.686	78.0±5.09
−40	1.58	0.65	0.094	23.9	0.65	0.038	9.51±12.41
		Experiment 67 (Two channels)					
		ACS method			MLE method		
V	K	P_o	P_I	β_I	P_o	P_I	β_I
mV				s^{-1}			s^{-1}
−25	1.16	0.45	0.514	232.7	0.46	0.570	258±24.4
−40	0.92	0.29	−0.251	—	0.32	0	0

maximum likelihood method, as shown on the right side of Table I. The estimated rate constants were used to produce P_I, and $P_o = \alpha_A/(\alpha_A + \alpha_I)$. For both experiments, the maximum likelihood and the ACS estimates for P_o agreed. Also, estimates of P_I agreed in most cases. However, at more hyperpolarized voltages, where both P_o and P_I were small, both methods were poor estimators of β_I, because it is much smaller than β_A. Although these estimates are less reliable (see above) than estimates at more depolarized voltages, it is clear from this table that β_I increases with depolarization.

Macroscopic Inactivation Is Not Entirely Explained by Either Open Time or Burst Duration

If we compare the semilogarithmic plots in Figs. 2 and 4*A*, it is clear that microscopic inactivation is sufficiently voltage dependent to be directly responsible for that observed in macroscopic inactivation. However, the magnitude of β_I is consistently larger than $1/\tau_h$. Since the open time is determined by both rate constants β_I and β_A (e.g., see Fig. 4*B*), it will be even shorter than $1/\beta_I$. Open time is therefore too brief to account for τ_h, as shown in Fig. 6*A*. Measured mean open times are plotted as filled symbols, and the uppermost solid line is τ_h (obtained from Fig. 2 and plotted on a linear scale here). Open time has very little voltage dependence in this range, since it is determined by both β_I and β_A, which have opposite voltage dependencies (Horn et al., 1984). The mean open time does, however, show a slight tendency to have larger values at intermediate voltages, as observed previously (Sigworth and Neher, 1980; Nagy et al., 1983; Horn et al., 1984). The lower bell-shaped curve in Fig. 6*A* is the predicted open time, using the theoretical curves of Figs. 4*A* and 5 for the values of β_I and β_A. The open times generally show less voltage dependence than this curve. This could be explained by saturation of β_I at depolarized voltages (see Discussion). Thus, the prediction of mechanism 1, that τ_h will have the same value as open time and $1/\beta_I$, is violated by our data.

Mechanism 2 predicts that mean burst duration will approximate the value

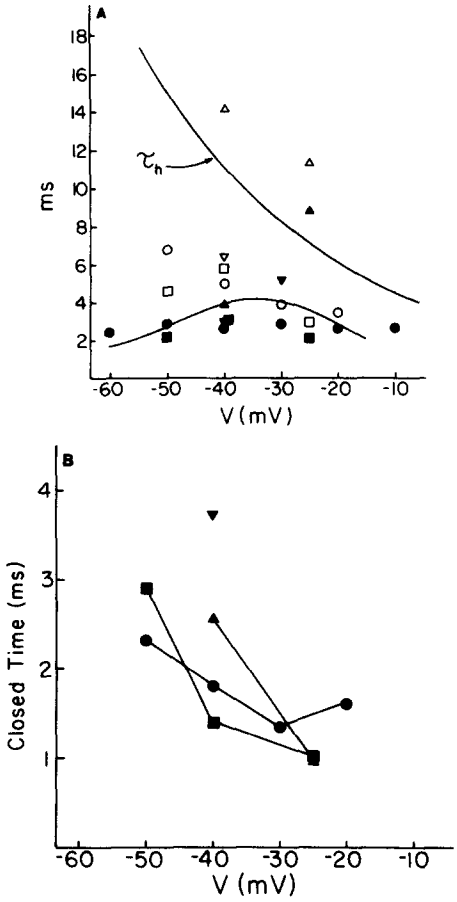

FIGURE 6. Mean open time, burst durations, and closed times vs. voltage. (*A*) Open times (filled symbols) from several single channel experiments are plotted on a linear scale together with burst durations (open symbols), calculated as described in the text. The predicted mean open time (lower curve) is calculated from the average linear regression values for β_I and β_A (Figs. 4*A* and 5). For comparison, τ_h (Fig. 2) is also shown (upper curve). (*B*) Mean closed times from the same experiments, calculated by the method in the Appendix. The symbols correspond with the same experiments plotted in *A* and Figs. 4 and 5.

and voltage dependence of τ_h. Burst duration can be measured directly in a patch with only one channel (Horn and Vandenberg, 1984), but must be estimated from all the rate constants in multichannel patches. The average number of openings in a burst, n, is obtained as described in Horn and Vandenberg (1984), and the mean burst duration is given by

$$\text{mean burst duration} = n(\text{mean open time}) + (n - 1)\ (\text{mean closed time})$$

(Colquhoun and Hawkes, 1981). The mean open time is given by the inverse of the sum of estimated rate constants leaving the open state. The Appendix outlines

the method we used for calculation of mean closed time in patches in which the rate constants of Scheme 1 were estimated by maximum likelihood analysis.

Fig. 6*B* plots the mean closed time obtained by this method and shows that it tends to decrease with depolarization, as in previous studies (Fukushima, 1981; Horn and Vandenberg, 1984). The number of openings per burst, n, also tended to decrease with depolarization, from ~1.6 at ~50 mV to ~1.2 at −20 mV (average value: 1.54). The decreases in both n and the mean closed time with depolarization contributed to a tendency for burst durations to decrease with depolarization, as shown by the open symbols in Fig. 6*A*. Consequently, the burst duration approaches the open time at depolarized potentials. This is expected from Fig. 4*B*, which shows that open channels tend to inactivate directly more often at depolarized potentials. The burst duration primarily consisted of time spent in the open state, with only brief closed times between openings. Although burst durations are, on the average, 1.76 times the mean open times, they are not as large or as voltage dependent as τ_h.

Voltage Dependence of Activation

The above results show that τ_h is larger than either open time or burst duration, eliminating mechanisms 1 and 2 from consideration, at least for voltages of less than −20 mV. The implication is that activation must play a role in macroscopic inactivation. We used two methods to calibrate the voltage dependence of activation, both involving macroscopic currents. We and others (Fukushima, 1981; Aldrich et al., 1983; Horn et al., 1984; Horn and Vandenberg, 1984) have previously shown that the first latency distribution is also a measure of activation and is highly voltage dependent. The methods we use here are fits of single exponentials to the slowest component of activation in trypsin-treated whole cells, which are devoid of inactivation, and to tail currents in control and trypsin-treated cells.

Trypsin, TPCK-treated to remove chymotrypsin activity, cleaves peptides specifically at lysine and arginine residues. It has the same specificity as alkaline proteinase-*b*, which is the active ingredient in pronase that removes inactivation in squid axon (Rojas and Rudy, 1976). In our hands, trypsin had two advantages over *N*-bromoacetamide, which we used previously to remove inactivation (Horn et al., 1984). First, it did not reduce the probability of opening, and second, it did not show evidence of slowing activation, as discussed below.

Fig. 7*A* shows three records from an outside-out patch after 15 min of exposure to trypsin in the pipette. By this time, the trypsin had removed most of the inactivation. The patch contained five channels, which were activated by step depolarizations to −40 mV. The long-duration openings are typical of channels in which inactivation is removed (Quandt and Narahashi, 1982; Patlak and Horn, 1982; Horn et al., 1984). The probability of each channel being open was quite high in the steady state, as shown by the average of 425 idealized records in Fig. 7*B*. The steady state probability of a channel being open in a trypsin-treated patch is at least as large as that in an untreated patch. Therefore, trypsin, unlike *N*-bromoacetamide, does not seem to induce hibernation (Horn et al., 1984).

Fig. 8 shows whole cell records in which trypsin in the pipette had removed

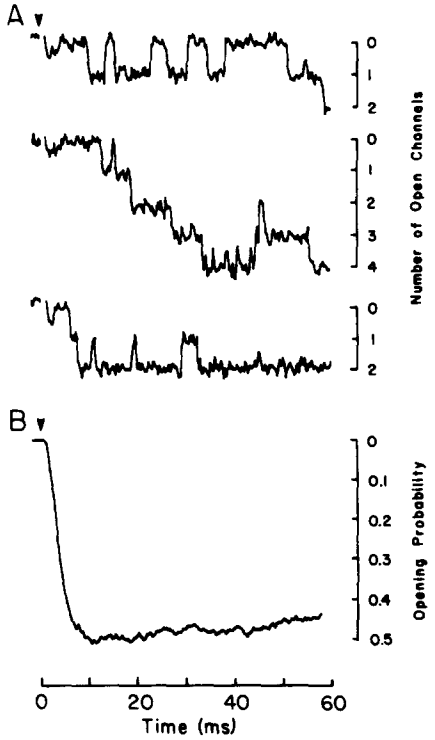

FIGURE 7. Single channel records from a trypsin-treated patch at −40 mV and their average probability of being open. (*A*) Three representative single channel records are shown, which were obtained after 15 min recording from an outside-out patch with five channels using a recording pipette containing 67 μg/ml trypsin. Inactivation was nearly completely removed after only 3 min exposure to trypsin. Currents were elicited during 60-ms test pulses to −40 mV from a holding potential of −110 mV. The interpulse interval was 1.5 s. (*B*) The probability of a single channel being open during the test pulse was derived by averaging 425 idealized single channel records and dividing by 5, the number of channels.

all evidence of inactivation. The complete removal of inactivation in whole cell experiments required a higher trypsin concentration and a prolonged treatment, usually 60–90 min, in comparison with 5–10 min in outside-out patches. Fig. 8 shows the macroscopic current in response to a series of step depolarizations (−40–0 mV) in 10-mV increments. The normalized peak currents from this cell and a control cell are plotted in the top panel of Fig. 9. The *I-V* relationships are comparable for the two conditions. The same data are plotted as normalized conductance (*G-V*) in the middle panel of Fig. 9. The trypsin-treated cell shows a slightly less voltage-dependent profile than the control cell, as in the comparison between pronased and control squid axon (Stimers et al., 1984). This may be due in part to the inaccuracy of peak currents as estimates of peak activation in control cells (French and Horn, 1983; Stimers et al., 1984). The lowermost panel of Fig. 9 plots the natural logarithm of $G/(G_{max} - G)$ vs. voltage. The slope of

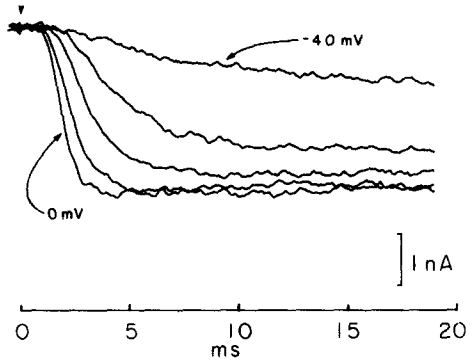

FIGURE 8. Trypsin-treated whole cell records for 20-ms voltage pulses to between −40 and 0 mV in 10-mV increments from a holding potential of −90 mV. The cell was internally perfused with trypsin by including 200 μg/ml trypsin in the recording pipette. Current traces, obtained 70 min after exposure to trypsin, are from 16 averaged whole cell records. The interpulse interval was 1.0 s.

this line at the foot of the activation process estimates its minimal voltage dependence (Almers, 1978). In the control and trypsin-treated cell, the values are 5.76 and 8.39 mV for an e-fold change, by comparison with ~7 mV for activation in pronase-treated squid axon (Stimers et al., 1984). These values are equivalent to minimal gating charges per channel of 4.3 and 3.0 electronic charges moving through the membrane field. This figure shows the reasonable correspondence between the conductance-voltage relationship in trypsin-treated and control cells.

Fig. 10 plots τ_m obtained from tail currents in control cells (open symbols) and another trypsin-treated whole cell (solid symbols), which shows that the latter time constants are somewhat bigger, by as much as threefold in the most extreme cases. It is not clear whether this is an expected effect of removing the inactivation gate, or a direct effect of trypsin on the activation kinetics. The mean advantage of using trypsin-treated cells, however, is the measurement of τ_m for activating depolarizations without the complications caused by inactivation. The half-filled symbols in Fig. 10 show such measurements. The bell-shaped curve of activation, drawn by eye, is replotted onto Fig. 2 to compare τ_m with τ_h. The prediction of mechanism 3 is that τ_m, which is the slowest time constant of activation, will correspond to τ_h. However, it falls below the latter over the whole voltage range. It does, however, have a similar slope of voltage dependence as τ_h. Note that if trypsin slows activation, the τ_m and τ_h curves from untreated channels would show a poorer correspondence than that shown in Fig. 2. The discrepancy between the curves in Fig. 2 suggests that mechanism 3 is incorrect. In other words, activation alone is insufficient to explain the rates and voltage dependence of inactivation.

Macroscopic Inactivation Depends on Activation and Burst Kinetics

In general, for a channel with only one open state, the probability that a channel is open at any time t, $P_{open}(t)$, is described by a convolution of the first latency

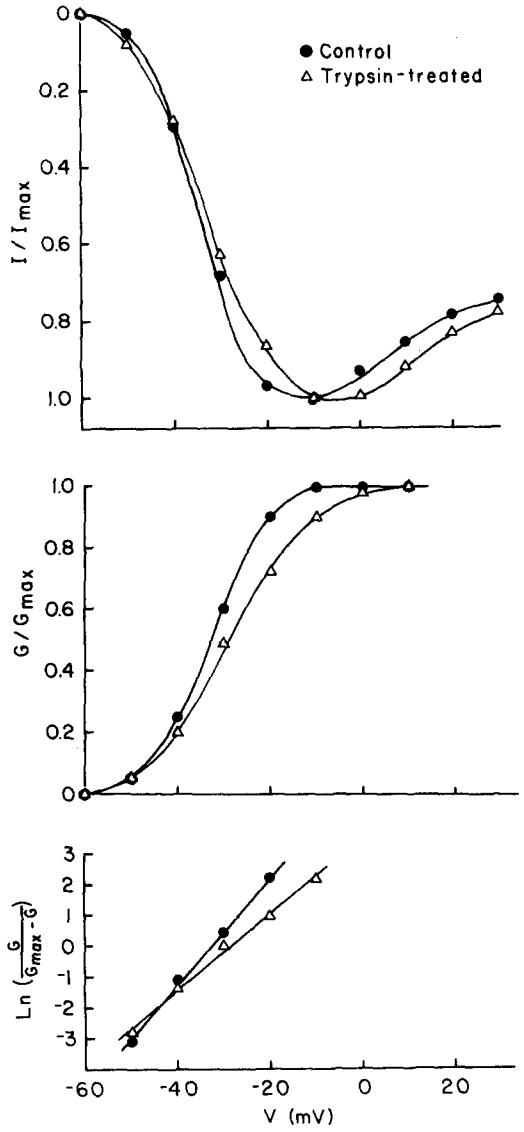

FIGURE 9. Current and conductance vs. voltage relationships for control (filled symbols) and trypsin-treated (open symbols) whole cell currents. Normalized peak currents (upper panel), normalized conductance (middle panel), and $\log[G/(G_{max} - G)]$ (lower panel) are plotted vs. voltage. Voltage steps were initiated from holding potentials of −80 (control) or −90 mV (trypsin-treated). Conductance was estimated using a linear *I-V* relationship (Horn et al., 1984) and assuming that maximal conductance was reached by +10 mV.

density and the autocorrelation function for the open state (i.e., the probability of a channel being open at time t given that it first opened at time zero; it is also called the burst open probability $M(t)$ in Horn and Vandenberg, 1984). If channels only open once and then inactivate directly, $P_{open}(t)$ can more simply be

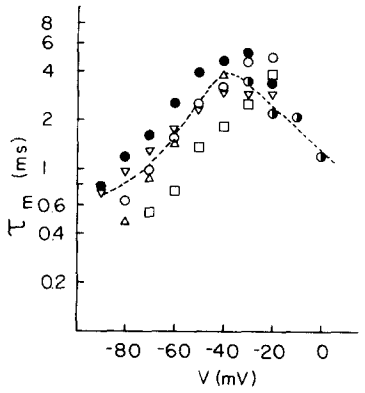

FIGURE 10. τ_m vs. voltage. τ_m, the slowest time constant for the macroscopic activation process, was obtained by fitting single exponentials to tail currents from whole cell recordings and to the activating currents in trypsin-treated whole cell recordings. Tail currents from control whole cell recordings (open symbols) were elicited at the peak of depolarizing prepulses (3–5 ms in the range 0 to +20 mV) for test pulses to the indicated voltage. Tail currents from trypsin-treated cell recordings (200 μg/ml, >70 min) were obtained following 8-ms prepulses to −20 mV. Single exponentials were also fit to the activation of trypsin-treated whole cell currents (half-filled symbols).

described as a convolution of the first latency density and $L(t)$, where $L(t)$ is the probability that a channel has not closed by time t given that it was open at time zero (Aldrich et al., 1983). A rigorous verification that reopenings of a single channel play an important role in macroscopic inactivation is that the mathematical convolution of the first latency density and $L(t)$ does not reproduce $P_{open}(t)$, as shown in Fig. 11 with data taken from the one-channel patch. The solid lines at −40 and −25 mV are plots of $P_{open}(t)$. The lowermost dotted line in each panel is the convolution of the first latency density and $L(t)$ (Aldrich et al., 1983), and the uppermost dotted line, which corresponds closely with $P_{open}(t)$, is the convolution of the first latency density with the autocorrelation. As noted previously, the burst duration approaches the open time at more depolarized potentials. Correspondingly, the convolution of $L(t)$ and first latency density is a better approximation of $P_{open}(t)$ at −25 than at −40 mV. However, it is clearly inadequate at both voltages. In addition to underestimating the amplitude of $P_{open}(t)$ at −40 mV, the shape of the falling phase of $P_{open}(t)$, which determines τ_h, is poorly approximated. Thus, we are left with mechanism 4 in this voltage range, which requires both activation and burst kinetics to account for the time course and voltage dependence of macroscopic inactivation.

Independent and Coupled Schemes Are Not Statistically Different

The above results show that the rate constants associated with both the activation and the inactivation processes contribute to macroscopic inactivation. Comparable rates in these pathways do not, however, address the question of coupling. If inactivation is independent of activation, the rate constant for inactivation is the

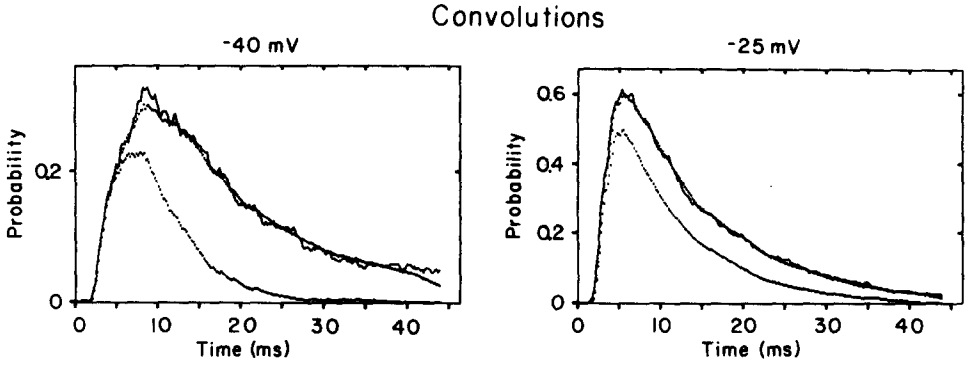

FIGURE 11. Convolutions and open probability for the one-channel patch. Convolutions of first latency density with $L(t)$ (lower dotted curve), or with burst open probability, i.e., autocorrelation (upper dotted curve), are plotted together with the probability of a channel being open (solid curve) during a voltage pulse to −40 or −25 mV. Convolutions were computed numerically from the measured density and distribution histograms. Note that the convolution of the first latency density and autocorrelation nearly superimposes on the probability of a channel being open, while the convolution of the first latency density and $L(t)$ underestimates the magnitude of the open probability and, at −40 mV, also underestimates τ_h.

same from each state in the activation pathway (Nonner, 1980; Goldman and Kenyon, 1982; French and Horn, 1983). A well-known model with independent inactivation is that of Hodgkin and Huxley (1952). Although this model is statistically inferior to more general models (Horn and Vandenberg, 1984), the rate constants along the activation pathway are themselves highly constrained. We have used likelihood ratio tests to examine unconstrained models. Because our models contain no more than five states, we could only test coupling with models having irreversible inactivation (Horn and Vandenberg, 1984) using either two or three closed states in the activation pathway.

The unconstrained model having three closed states is shown below.

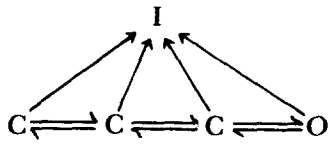

(Scheme 2)

All 10 rate constants are free parameters in this coupled model (model 10 in Table II of Horn and Vandenberg, 1984). Using data from the single channel patch, this model was compared with a seven-parameter independent model in which all rate constants entering the inactivated state were equal. A likelihood ratio test for this comparison produced a chi-square (and corresponding degrees of freedom) value of 8.81 (6) with a corresponding P value of ~0.2. Therefore, we find no statistical evidence for a difference between the coupled and independent version of Scheme 2. A similar test was applied to a model with two closed states in the activation pathway. In this case, the chi-square (and degrees

of freedom) value was 3.61 (4), $P \sim 0.5$. Thus, our data and analysis fail to show direct evidence for coupling.

DISCUSSION

The macroscopic sodium currents in GH_3 cells are qualitatively similar to those in other preparations, in terms of showing highly voltage-dependent activation and inactivation. We examined several possible mechanisms that could, in principle, explain the voltage dependence of macroscopic inactivation. Our results suggest that both activation and microscopic inactivation play significant roles in determining the voltage dependence of τ_h, as discussed below.

Comparison of Whole Cell and Single Channel Currents

In the previous paper (Horn and Vandenberg, 1984), we confirmed the quality of the maximum likelihood estimates of rate constants and kinetic models by using the estimates to make several predictions of histograms and conditional probabilities. In this paper, we can take this another step forward and use these rate constants to generate macroscopic currents. The rate constants for the five-state model (Scheme 1) were estimated for the nontruncated data (Horn and Vandenberg, 1984) from our single channel patch at two voltages, −40 and −25 mV. We then assumed that all rate constants were exponential functions of voltage, and simulated macroscopic currents by calculating $P_{open}(t)$ and multiplying this by the single channel current-voltage relationship (Horn et al., 1984). The resulting currents did not provide satisfactory comparisons with our measured macroscopic currents, largely because the currents above −20 mV were too small and too fast. By trial and error, we found that the principal reason for the discrepancy was β_1. If β_1 were made less voltage dependent at depolarized voltages, the simulated currents were better approximations to actual whole cell currents, as seen by a comparison of Fig. 12*A* with Fig. 1. The relationship between β_1 and voltage used to produce these whole cell currents is shown in Fig. 12*B*. The type of saturation seen in Fig. 12*B* has been observed previously for rate constants estimated from endplate currents (Neher and Stevens, 1979; Durant and Horn, 1984) and is expected when the dipole moment between the open state and the inactivated state is a function of membrane potential (Neher and Stevens, 1979). It is interesting that the inactivation rate constant β_h of Hodgkin and Huxley (1952) also saturated in the same fashion as our β_1. We found that simulations in which β_1 was constrained to be voltage independent over the entire range were completely unsatisfactory predictors of macroscopic currents. The predicted currents in this case only showed a slight voltage dependence of macroscopic inactivation at potentials more depolarized than −30 mV, but in the opposite direction from the whole cell currents. That is, the predicted τ_h increased slightly with voltage above −30 mV and approached $1/\beta_1$.

The postulated saturation of β_1 at depolarized potentials has an interesting implication. Since the open time at such potentials is primarily determined by β_1 (Fig. 4*B*), the open time should show very little voltage dependence at potentials above 0 mV. This suggests that open time, burst time, and τ_h will converge here

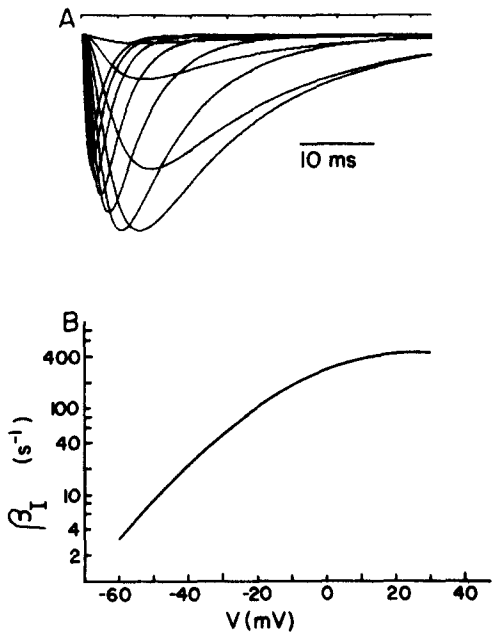

FIGURE 12. Macroscopic current simulation. (*A*) Macroscopic currents were simulated for voltage steps from −50 to +30 mV in 10-mV increments by extrapolating the rate constants obtained by maximum likelihood analysis of nontruncated current records from the one-channel patch at −40 and −25 mV. Rate constants were assumed to be exponential functions of voltage, except that β_I was given a less steep voltage dependence at depolarized voltages as shown in *B*.

(see Fig. 6*A*). Therefore, at sufficiently depolarized voltages, τ_h and $1/\beta_I$ will be the same, in accordance with mechanism 1, and τ_h will become less voltage dependent here, a phenomenon apparent in Fig. 2 and also seen in squid axon (Bezanilla and Armstrong, 1977).

Further support for mechanism 1 at depolarized potentials is that the first latency distribution becomes very fast with depolarization (Aldrich et al., 1983; Horn et al., 1984; Horn and Vandenberg, 1984), while the open time changes very little. Fig. 13*A* shows simulated first latency densities for voltage steps from a holding potential to a series of voltages (from −50 up to +20 mV in 10-mV increments), using the same model and parameters for predicting macroscopic currents. A comparison of these first latency densities with the macroscopic currents in Fig. 12*A* shows that the overlap between the first latency density and macroscopic inactivation is only significant at hyperpolarized voltages. (The same is obvious from the data in Horn and Vandenberg, 1984.) For example, at −50 mV only 51% of channels have opened for the first time when the macroscopic current has reached its peak. Therefore, at this voltage the times when channels first enter the open state are distributed throughout the decay phase of the current. The pathway to inactivation at this voltage is expected to involve significant bursting (see the description of mechanism 4, above). However, at −20 mV 87% of channels have reached the open state by the time the macro-

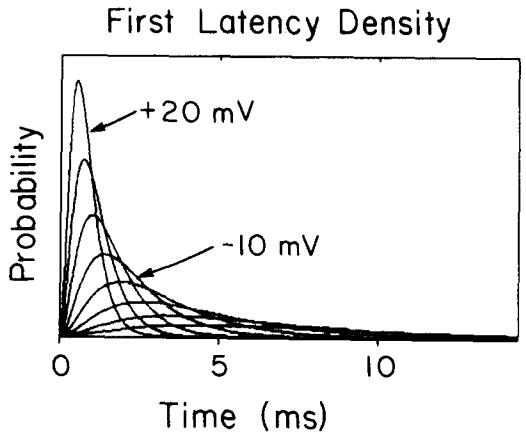

FIGURE 13. First latency density simulation. First latency densities were simulated for voltage steps from −50 to +20 mV in 10-mV increments as in Fig. 12.

scopic current has reached its peak. In this case, the time course of macroscopic inactivation is primarily determined by burst kinetics, as suggested by mechanism 2 (see above). At voltages >0 mV, the first latency density approaches a Gaussian shape (cf. Rubinson, 1982) and is much faster than macroscopic inactivation. Presumably channels open only once in this voltage region (see Fig. 4*B*), as described by mechanism 1. Accordingly, our simulated macroscopic currents have a measured τ_h at these voltages that approximately equals $1/\beta_I$. Thus, depolarization gradually transforms the interaction between activation and inactivation from mechanisms 4 to 2 to 1. In our experiments, mechanism 3 never prevails, because we never see single openings at the same voltages where the first latency distribution is slow.

The stimulated currents of Fig. 12*A* are not identical to our measured macroscopic currents. The two main discrepancies are that they are somewhat slower and that the peak current-voltage relationship is shifted in the hyperpolarizing direction. The latter phenomenon is commonly observed in comparisons between currents of outside-out patches and whole cells (Fenwick et al., 1982; Marty and Neher, 1983; Fernandez et al., 1984; Fig. 2 of this paper). The former discrepancy is characteristic of the variability between channels in our experiments. Both problems may be due to alterations of channels in the outside-out patch configuration (Trautmann and Siegelbaum, 1983), or may be representative of the normal heterogeneity in the population of individual channels. This heterogeneity is notable in Figs. 4*A* and 6*A*, which show maximum likelihood estimates of β_I, open time, and burst duration. By contrast, estimates of β_A, the closing rate constant, are less variable between cells. Our experiments do not address whether heterogeneity from patch to patch corresponds with heterogeneity among cells, because no two patches were obtained from the same cell.

Inherent Voltage Dependence of Microscopic Inactivation

An inherent voltage dependence of inactivation has previously been suggested from single channel studies (Sigworth and Neher, 1980; Horn et al., 1984) and

from recent experiments involving pronase-treated squid axons (Stimers et al., 1984). The voltage dependence of β_1 suggests that depolarization increases the rate of closing of an inactivation gate. If the gate is perceived as the charged "inactivation plug" in the conceptual model of Armstrong and Bezanilla (1977), then its binding site is located in the membrane field. This process is reminiscent of the voltage-dependent binding of cationic open channel blockers (e.g., see Armstrong, 1969; Adams, 1976; Neher and Steinbach, 1978; Miller, 1982). A block of sodium channels from the intracellular membrane surface has also been postulated for a number of cationic molecules (for reviews, see Brodwick and Eaton, 1982; Yeh, 1982). Some of these molecules, when added to the internal perfusate, mimic inactivation in pronased axons, which suggests the possibility that the inactivation gate itself acts like a typical extrinsic channel blocker. If this conception is correct, the saturating voltage dependence of β_1 suggests that the gate cannot achieve the binding rates of a freely diffusing open channel blocker. This is a reasonable expectation for a sterically constrained macromolecule.

Our statistical tests fail to show a significant coupling between activation and inactivation. This may be a simple failure to resolve the coupling with our method of analysis. However, it suggests the possibility that the inactivation gate can bind to its site without regard to the state of the activation machinery. This idea is consistent with the notion that closed channels can inactivate (Bean, 1981; Horn et al., 1981; Aldrich et al., 1983; Patlak, 1983; Aldrich and Stevens, 1983; Horn and Vandenberg, 1984), but is inconsistent with the usual conception of coupling, in which the rate of microscopic inactivation increases as activation proceeds toward channel opening. It is important to stress that our failure to find coupling is not proof of independence. Further analysis and experiments will be required to clarify this point, in light of the vast evidence in support of coupling (Armstrong, 1981; Bezanilla, 1982; French and Horn, 1983).

Comparisons with Other Studies of Sodium Channel Gating

Perhaps the most notable discrepancy between our results and previous work is that Aldrich et al. (1983) and Aldrich and Stevens (1983), primarily using cell-attached patch recording in neuroblastoma cells, found that single channels usually open at most one time during a depolarization and close directly into an inactivated state. Consequently, open time is equivalent to $1/\beta_1$ in the major voltage range of activation. Furthermore, β_1 in this range is independent of voltage. The difference between our respective conclusions cannot be attributed to our methods of data analysis, because we reach the same results using their method of analysis (Table I). The discrepancy is primarily due to a difference in the data. We will briefly examine three possible explanations for this difference.

(*a*) The difference may be due to a difference in the type of cell. This seems unlikely to us, because we have also seen evidence of frequent reopenings in neuroblastoma cells (N1E-115) in unpublished experiments under the same conditions as used here. Furthermore, Aldrich et al. (1983) reported that they confirmed their conclusions using GH_4 cells, a close relative of GH_3 cells.

(*b*) The difference could be explained by our ability to resolve brief closing at cool temperatures. The kinetics of gating in our experiments were slowed by

cooling to 9.3°C, whereas Aldrich et al. (1983) show most results in the range of 16–22°C. The temperature difference could also have a more direct significance by changing the relative values of rate constants in the kinetic scheme. This is the expected effect of temperature, since the enthalpies of individual transitions are not expected to be the same (Horn, 1984). However, temperature does not seem to explain the difference between our results, because recent experiments by us (unpublished) at room temperature show a similar pattern of frequent reopenings, and experiments by Aldrich and Stevens (personal communication) do not show such behavior at cool temperatures.

(*c*) The process of excision of a patch may alter the properties of the channels by comparison with channels functioning in a cell-attached patch (Cachelin et al., 1983; Trautmann and Siegelbaum, 1983). The alteration could be due to such factors as a change of internal surface potential, dilution of some cytoplasmic component, or damage to the channels. Alternatively, the differences may reflect a change in the functional properties of channels because of the extent to which they are phosphorylated (Costa et al., 1982). The fact that averaged single channel records in excised patches correspond well with whole cell measurements (Fig. 2; also see Fernandez et al., 1984) suggests that channel damage caused by excision is not a significant factor. Our data would tend to correspond better with those of Aldrich et al. (1983) if the saturating voltage dependence of β_I, as depicted in Fig. 12*B*, were shifted in the hyperpolarized direction with no change in β_A. This is the opposite effect on surface potential expected for the replacement of intracellular polyanions with intracellular solution containing F^- (Dani et al., 1983), but could, for example, be due to a direct effect of F^- on the sodium channel. Direct effects of F^- on sodium channels have been suggested previously by Chandler and Meves (1970) in squid axons and by Takahashi and Yoshii (1978) in tunicate eggs. Since we perfuse the whole cells with CsF, a comparison of single channel and whole cell records requires us to perfuse the patches. We have not investigated the possibility of a difference between inside-out and outside-out patches.

Although the possibility of a difference between excised and cell-attached patches seems reasonable to us, multiple reopenings of sodium channels are very apparent in cell-attached recordings in tunicate eggs (Fukushima, 1981). As in our experiments, the reopenings in this preparation decrease with depolarization (Fukushima, 1981). We are currently investigating the properties of sodium channels in cell-attached patches from GH_3 cells in order to clarify the above-mentioned discrepancies.

Comparisons with Gating Current Experiments

Our kinetic models show a voltage dependence of microscopic inactivation, in contrast with conclusions reached from the analysis of gating current experiments (Armstrong, 1981; French and Horn, 1983). One argument against a voltage dependence to this transition is that gating current does not usually show a component with the same time course as macroscopic inactivation (but see Swenson, 1983). However, when gating currents are simulated using the rate constants estimated from our single channel data (Table II and Fig. 14*A*), then

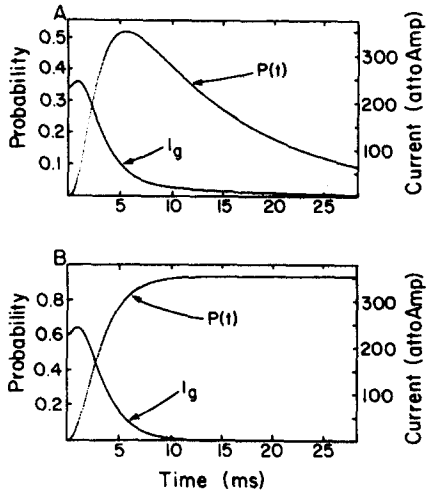

FIGURE 14. Predicted gating current and open probability at −25 mV before (*A*) and after (*B*) removal of inactivation. Gating currents were estimated from the rate constants (Table II) derived from the nontruncated current records from the one-channel patch at −40 and −25 mV assuming an exponential voltage dependence of the rate constants. (*B*) Inactivation was eliminated by making the rate constants for entering the inactivated state equal to zero. Note that only slight differences in the late phase of the predicted gating current result from removal of inactivation. (1 attoamp = 1 quintillionth ampere.)

in spite of the large voltage dependence of microscopic inactivation, this component of gating current is quite small. Furthermore, the removal of inactivation has very little effect on the time course or amplitude of the gating current (Fig. 14*B*), which agrees with experiments in squid axon (Gilly et al., 1981; Stimers et al., 1984). Thus, the absence of a conspicuous component of gating current

TABLE II

Estimates of Rate Constants and Gating Charges

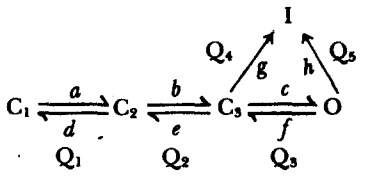

Rate constants (s^{-1}) at −25 mV
$a^* = b^* = 1{,}204$, $c = 634$, $d = e = 165$
$f = 35.5$, $g = 192$, $h = 77.9$
Equivalent charge for above transitions
$Q_1 = Q_2 = 1.21$, $Q_3 = 4.24$
$Q_4 = 0.01$, $Q_5 = 3.62$

* The rate constants *a* and *b* were increased by 30% over those estimated to obtain a better fit to the rising phase of averaged current records.

associated with macroscopic inactivation is consistent with a kinetic scheme with voltage-dependent microscopic inactivation. Note that Fig. 14 represents the average gating current for a single channel. The actual gating current for one trial in a Markov gating scheme theoretically will be a series of delta functions.

Our estimates of the voltage dependence of the transitions in Scheme 1 are shown in Table II, with the assumption of an exponential dependence of the rate constants on membrane potential. The estimates, it should be stressed, are from one patch, and are not identical to estimates from other patches which, in general, showed less voltage dependence for the O → I transition. The absolute voltage dependence and the relative magnitudes of rate constants at −25 mV in this scheme are somewhat similar to the model of Armstrong and Gilly (1979), based on experiments in squid axon, except that they assume only minimal voltage dependence to the O → I transition. Recent experiments by Stimers et al. (1984) show that some voltage dependence is necessary for this transition in squid axon. In addition to the lack of detectable gating current caused by inactivation, the estimated gating current in Fig. 14 is instructive in other ways. First, the most prominent phase of the current has a time course similar to that of the sigmoidal activation of channels, which is equivalent to the intermediate component of Armstrong and Gilly (1979). Second, the peak average gating current for a channel at −25 mV is ~240 aA. A comparison of the amplitudes of macroscopic and single channel currents shows that GH_3 cells often have $>10^5$ channels, giving a peak gating current of 24 pA. Although this is marginally resolvable, the kinetics at more depolarized potentials, and especially at warmer temperatures, will be much faster and therefore the gating currents will have a larger amplitude. This estimate demonstrates the potential for obtaining gating currents, macroscopic currents, and single channel currents in the same preparations. The combination of all three types of measurement has not been possible for sodium channels in classical preparations such as squid axon and should greatly enhance the possibility of refining an accurate kinetic model.

APPENDIX

Calculation of Mean Closed Time

We assume the kinetic model Scheme 1 (above) in which the inactivated state I is absorbing. Closed time for a single channel is defined as the time between a closing event and a subsequent reopening. This definition excludes the situation of a channel closing and never reopening. Calculation of closed time is obtained by setting the initial condition that the channel is in C_3 at time zero and making the open state absorbing (Colquhoun and Hawkes, 1981; Horn and Lange, 1983). Thus, the appropriate kinetic scheme is

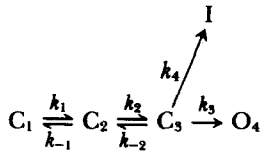

where C_1, C_2, and C_3 are closed states, and O_4 is the open state. We would like to determine the mean waiting time $\bar{W}_{34}$ for the next visit to the open state following closing,

where $\bar{W}_{ij}$ is the mean waiting time for the first transition to state j starting in state i. Since channels that enter the inactivated state I do not contribute to the mean waiting time, $\bar{W}_{34}$ is made up only of channels that pass directly to O_4 from C_3 or which go to the closed states C_2 and C_1 before making the transition from C_3 to O_4. A channel in C_1 or C_2 must ultimately return to C_3, from which it will open, inactivate, or return to C_2. If the population of channels is divided according to the number, n, of cycles that are made from C_3 to C_2 and back to C_3 before opening, then the probabilities of these pathways and their durations are:

Pathway	Probability	Time
$C_3 \rightarrow O_4$	k_3/θ	$1/\theta$
$C_3 \rightarrow C_2 \rightarrow C_3 \rightarrow O_4$ $\uparrow\downarrow$ C_1	$(k_{-2}/\theta)(k_3/\theta)$	$(2/\theta) + \bar{W}_{23}$
$(C_3 \rightarrow C_2 \rightarrow C_3)_n \rightarrow O_4$ $\uparrow\downarrow$ C_1	$(k_{-2}/\theta)^n(k_3/\theta)$	$(n+1)/\theta + n(\bar{W}_{23})$

where $1/\theta = 1/(k_3 + k_4 + k_{-2})$ = mean channel lifetime in C_3, and

$$\bar{W}_{23} = [\text{Prob}(C_2 \rightarrow C_3)](\text{mean lifetime in } C_2) + [\text{Prob}(C_2 \rightarrow C_1)][(\text{mean lifetime in } C_2) + (\text{mean lifetime in } C_1) + \bar{W}_{23}];$$

$$\bar{W}_{23} = \frac{k_2}{(k_2 + k_{-1})}\frac{1}{(k_2 + k_{-1})} + \frac{k_{-1}}{(k_2 + k_{-1})}\left[\frac{1}{(k_2 + k_{-1})} + \frac{1}{k_1} + \bar{W}_{23}\right]; = 1/k_2 + k_{-1}/k_1k_2.$$

The proportion of total channels contributing to the waiting time $\bar{W}_{34}$ is just the sum of the probabilities for the possible pathways from C_3 to O_4, and is equal to $k_3/(k_3 + k_4)$.

Thus, the mean closed time $\bar{W}_{34}$ is:

$$\bar{W}_{34} = \frac{\sum_{n=0}^{\infty} \{(\text{mean time for pathway}_n)[\text{Prob}(\text{channel takes pathway}_n)]\}}{(\text{proportion of channels starting in } C_3 \text{ that contribute to closed time})},$$

where pathway_n is the pathway from C_3 to O_4 with n cycles between C_3 and C_2.

$$W_{34} = (k_3 + k_4)/k_3\{(k_3/\theta)(1/\theta)[1 + 2(k_{-2}/\theta) + 3(k_{-2}/\theta)^2 + \ldots + (n+1)(k_{-2}/\theta)^n + \ldots] + (k_3/\theta)(1/k_2 + k_{-1}/k_1k_2)[(k_{-2}/\theta) + 2(k_{-2}/\theta)^2 + 3(k_{-2}/\theta)^3 + \ldots + n(k_{-2}/\theta)^n + \ldots]\}$$

$$= \frac{(k_3 + k_4)}{k_3}\left\{\frac{k_3}{\theta^2}\frac{1}{[1 - (k_{-2}/\theta)]^2} + \frac{k_3}{\theta}\left(\frac{1}{k_2} + \frac{k_{-1}}{k_1k_2}\right)\frac{(k_{-2}/\theta)}{[1 - (k_{-2}/\theta)]^2}\right\}$$

$$= \frac{1}{(k_3 + k_4)} + \frac{k_{-2}}{k_2(k_3 + k_4)} + \frac{k_{-1}k_{-2}}{k_1k_2(k_3 + k_4)}.$$

The mean closed time consists of the sum of three terms. The first is the mean time spent in C_3, the second is the mean time in C_2, and the third is the mean dwell time in C_1. The fraction $1/(k_3 + k_4)$ is the mean lifetime in state C_3 if k_{-2} is zero. The ratios k_{-2}/k_2

and $k_{-1}k_{-2}/k_1k_2$ represent the fraction of channels dwelling in states C_2 and C_1 compared with C_3.

We are grateful to Drs. Richard Aldrich and Charles Stevens for illuminating discussions and to Drs. Francisco Bezanilla and Joseph Stimers for offering criticisms of the manuscript. The title of this paper was suggested to us by Dr. Aldrich.
Supported by National Institutes of Health grants NS 703-01 and NS 186-08, and by National Science Foundation grant PCM 76-20605 to R.H. C.V. was supported by Muscular Dystrophy Association and National Institutes of Health postdoctoral fellowships.

Original version received 28 March 1984 and accepted version received 13 June 1984.

REFERENCES

Adams, P. R. 1976. Drug blockade of open end-plate channels. *J. Physiol. (Lond.).* 260:531–552.

Aldrich, R. W., D. P. Corey, and C. F. Stevens. 1983. A reinterpretation of mammalian sodium channel gating based on single channel recording. *Nature (Lond.).* 306:436–441.

Aldrich, R. W., and C. F. Stevens. 1983. Inactivation of open and closed sodium channels determined separately. *Cold Spring Harbor Symp.* 48:147–153.

Almers, W. 1978. Gating currents and charge movements in excitable membranes. *Rev. Physiol. Biochem. Pharmacol.* 82:6–190.

Armstrong, C. M. 1969. Inactivation of the potassium conductance and related phenomena caused by quaternary ammonium ion injection in squid axons. *J. Gen. Physiol.* 54:553–575.

Armstrong, C. M. 1981. Sodium channels and gating currents. *Physiol. Rev.* 61:644–683.

Armstrong, C. M., and F. Bezanilla. 1977. Inactivation of the sodium channel. II. Gating current experiments. *J. Gen. Physiol.* 70:567–590.

Armstrong, C. M., and W. F. Gilly. 1979. Fast and slow steps in the activation of sodium channels. *J. Gen. Physiol.* 74:691–711.

Bean, B. P. 1981. Sodium channel inactivation in the crayfish giant axon. Must channels open before inactivating? *Biophys. J.* 35:595–614.

Bezanilla, F. 1982. Gating charge movements and kinetics of excitable membrane proteins. *In* Proteins of the Nervous System: Structure and Function. B. Haber, J. R. Perez-Polo, and J. D. Coulter, editors. Alan R. Liss, Inc., New York. 3–16.

Bezanilla, F., and C. M. Armstrong. 1977. Inactivation of the sodium channel. I. Sodium current experiments. *J. Gen. Physiol.* 70:549–566.

Brodwick, M. S., and D. C. Eaton. 1982. Chemical modification of excitable membranes. *In* Proteins in the Nervous System: Structure and Function. B. Haber, J. R. Perez-Polo, and J. D. Coulter, editors. Alan R. Liss, Inc., New York. 51–72.

Cachelin, A. B., J. E. De Peyer, S. Kokuban, and H. Reuter. 1983. Sodium channels in cultured cardiac cells. *J. Physiol. (Lond.).* 340:389–401.

Chandler, W. K., and H. Meves. 1970. Evidence for two types of sodium conductance in axons perfused with sodium fluoride solution. *J. Physiol. (Lond.).* 211:653–678.

Colquhoun, D., and A. G. Hawkes. 1977. Relaxation and fluctuations of membrane currents that flow through drug-operated channels. *Proc. R. Soc. Lond. B Biol. Sci.* 199:231–262.

Colquhoun, D., and A. G. Hawkes. 1981. On the stochastic properties of single ion channels. *Proc. R. Soc. Lond. B Biol. Sci.* 211:205–235.

Colquhoun, D., and B. Sakmann. 1981. Fluctuations in the microsecond time range of the current through single acetylcholine receptor ion channels. *Nature* (*Lond.*). 294:464–466.

Costa, M. R. C., J. E. Casnellie, and W. A. Catterall. 1982. Selective phosphorylation of the subunit of the sodium channel by cAMP-dependent protein kinase. *J. Biol. Chem.* 14:7918–7921.

Dani, J. A., J. A. Sanchez, and B. Hille. 1983. Lyotropic anions. Na channel gating and Ca electrode response. *J. Gen. Physiol.* 81:255–281.

Durant, N. N., and R. Horn. 1984. A nondepolarizing neuromuscular blocking agent with a novel effect on endplate conductance. *J. Pharmacol. Exp. Ther.* 228:567–572.

Fenwick, E. M., A. Marty, and E. Neher. 1982. Sodium and calcium channels in bovine chromaffin cells. *J. Physiol.* (*Lond.*). 331:599–635.

Fernandez, J., A. P. Fox, and S. Krasne. 1984. Membrane patches and whole-cell membranes: a comparison of electrical properties in rat clonal pituitary (GH_3) cells. *J. Physiol.* (*Lond.*). In press.

French, R. J., and R. Horn. 1983. Sodium channel gating: models, mimics, and modifiers. *Annu. Rev. Biophys. Bioeng.* 12:319–356.

Fukushima, Y. 1981. Identification and kinetic properties of the current through a single Na^+ channel. *Proc. Natl. Acad. Sci. USA.* 78:1274–1277.

Gilly, W. F., R. P. Swenson, and C. M. Armstrong. 1981. Sodium channel activation in pronased squid axons: the slow last step. *In* VII International Biophysics Congress. Mexico City, Mexico. 330.

Goldman, L., and J. L. Kenyon. 1982. Delays in inactivation development and activation kinetics in *Myxicola* giant axons. *J. Gen. Physiol.* 80:83–102.

Hodgkin, A. L., and A. F. Huxley. 1952. A quantitative description of the membrane current and its application to conduction and excitation in nerve. *J. Physiol.* (*Lond.*). 117:500–544.

Horn, R. 1984. Gating of channels in nerve and muscle: a stochastic approach. *In* Ion Channels: Molecular and Physiological Aspects. W. D. Stein, editor. Academic Press, Inc., New York. In press.

Horn, R., and M. S. Brodwick. 1980. Acetylcholine-induced current in perfused rat myoballs. *J. Gen. Physiol.* 75:297–321.

Horn, R., and K. Lange. 1983. Estimating kinetic constants from single channel data. *Biophys. J.* 43:207–223.

Horn, R., J. Patlak, and C. Stevens. 1981. Sodium channels need not open before they inactivate. *Nature* (*Lond.*). 291:426–427.

Horn, R., and C. A. Vandenberg. 1984. Statistical properties of single sodium channels. *J. Gen. Physiol.* 84:505–534.

Horn, R., C. A. Vandenberg, and K. Lange. 1984. Statistical analysis of single sodium channels. Effects of *N*-bromoacetamide. *Biophys. J.* 45:323–335.

Marty, A., and E. Neher. 1983. Tight-seal whole-cell recording. *In* Single-Channel Recording. B. Sakmann and E. Neher, editors. Plenum Press, New York. 107–122.

Miller, C. 1982. *Bis*-quaternary ammonium blockers as structural probes of the sarcoplasmic reticulum K^+ channel. *J. Gen. Physiol.* 79:869–891.

Nagy, K., T. Kiss, and D. Hof. 1983. Single Na channels in mouse neuroblastoma cell membrane. Indications for two open states. *Pflügers Arch. Eur. J. Physiol.* 399:302–308.

Neher, E., and J. H. Steinbach. 1978. Local anaesthetics transiently block currents through single acetylcholine-receptor channels. *J. Physiol.* (*Lond.*). 277:153–176.

Neher, E., and C. F. Stevens. 1979. Voltage-driven conformational changes in intrinsic membrane proteins. *In* The Neurosciences. Fourth Study Program. MIT Press, Cambridge, MA. 623–629.

Nonner, W. 1980. Relations between the inactivation of sodium channels and the immobilization of gating charge in frog myelinated nerve. *J. Physiol. (Lond.)*. 299:573–603.

Oxford, G. S. 1981. Some kinetic and steady state properties of sodium channels after removal of inactivation. *J. Gen. Physiol.* 77:1–22.

Patlak, J. 1983. Conditional probability measurements on two models of Na channel kinetics. *In* The Physiology of Excitable Cells. A. Grinnell and W. Moody, editors. Alan R. Liss, Inc., New York. 165–180.

Patlak, J., and R. Horn. 1982. The effect of *N*-bromoacetamide on single sodium channel currents in excised membrane patches. *J. Gen. Physiol.* 79:333–351.

Powell, M. J. D. 1978. Fast algorithm for nonlinearity constrained optimization calculations. *In* Numerical Analysis. G. A. Watson, editor. Lecture Notes in Mathematics No. 630, Springer-Verlag, Berlin. 144–157.

Quandt, F. N., and T. Narahashi. 1982. Modification of single Na^+ channels by batrachotoxin. *Proc. Natl. Acad. Sci. USA.* 79:6732–6736.

Rao, C. R. 1973. Linear Statistical Inference and Its Applications. Second edition. John Wiley & Sons, New York. 625 pp.

Rojas, E., and B. Rudy. 1976. Destruction of the sodium conductance inactivation by a specific protease in perfused nerve fibers from *Loligo*. *J. Physiol. (Lond.)*. 262:477–494.

Rubinson, K. A. 1982. The sodium currents of nerve under voltage clamp as heterogeneous kinetics. A model that is consistent with possible kinetic behavior. *Biophys. Chem.* 15:245–262.

Sigworth, F. J. 1983. Electronic design of the patch clamp. *In* Single-Channel Recording. B. Sakmann and E. Neher, editors. Plenum Press, New York. 3–35.

Sigworth, F. J., and E. Neher. 1980. Single Na^+ channel currents observed in cultured rat muscle cells. *Nature (Lond.)*. 287:447–449.

Stimers, J. R., F. Bezanilla, and R. E. Taylor. 1984. Sodium channel activation in squid axon. Steady state properties. *J. Gen. Physiol.* In press.

Swenson, R. P., Jr. 1983. A slow component of gating current in crayfish giant axons resembles inactivation charge movement. *Biophys. J.* 41:245–249.

Takahashi, K., and M. Yoshii. 1978. Effects of internal free calcium upon the sodium and calcium channels in the tunicate egg analyzed by the internal perfusion technique. *J. Physiol. (Lond.)*. 279:519–549.

Trautmann, A., and S. A. Siegelbaum. 1983. The influence of membrane isolation on single acetylcholine-channel current in rat myotubes. *In* Single-Channel Recording. B. Sakmann and E. Neher, editors. Plenum Press, New York. 473–480.

Yeh, J. 1982. A pharmacological approach to the structure of the Na channel in squid axon. *In* Proteins in the Nervous System: Structure and Function. B. Haber, J. R. Perez-Polo, and J. D. Coulter, editors. Alan R. Liss, Inc., New York. 17–49.